IMPACT OF ANNEALING TEMPERATURE ON OPTICALPARAMETERS OF $La_{0.25}Sr_{0.75}MnO_3$ NANOCRYSTALLITES

Mohd Abdul Shukur[1,2], K. Vijaya Kumar[1*], G. Narsinga Rao[3]

Article History: **Received:** 03.12.2022 **Revised:**15.01.2023 **Accepted:** 20.02.2023.

Abstract: Lanthanum doped Strontium manganites $La_{0.25}Sr_{0.75}MnO_3$ perovskite nanocrystallites were synthesized by combustion method followed by annealed at the temperatures 600, 800, 1000 and 1200℃ for 6 hours. These nanocrystallites were analyzed using X ray diffractometer (XRD) and UV -Vis spectrometer. From the XRD patterns, it was confirmed the formation of Rhombohedral structure (space group $R\bar{3}C$) without any impurity peaks. The average crystallite size was seen to increase gradually as function of annealing temperature from 13.6 to 22.7nm. From UV-Vis spectra, the calculated optical energy gap of $La_{0.25}Sr_{0.75}MnO_3$ nanocrystalline as reduced from 3.83 to 2.64eV with the annealed temperature, reveals that the $La_{0.25}Sr_{0.75}MnO_3$ nanocrystallites are semiconductors in nature. Hence $La_{0.25}Sr_{0.75}MnO_3$ nanocrystallites annealed at different temperature showed novel structural and optical properties.

Keywords: Perovskite manganite, Band gap, Refractive index.

1Department of Physics, JNTUH University College of Engineering Rajanna Sircilla, Agraharam, Rajanna Sircilla-District, 505301, Telangana, India.

2Department of Physics, SRR Government Arts & Science College (Autonomous), Karimnagar, 505001, Telangana, India

3Department of Physics, Marri Laxman Reddy Institute of Technology and Management, Dundigal, Hyderabad 500043, Telangana, India.

*Corresponding Author: kvkphd@gmail.com

DOI: 10.48047/ecb/2023.12.sa1.506

INTRODUCTION

Perovskite Lanthanum manganite with a composition of $La_{1-x}A_xMnO_3$ (A = Sr, Ba, Ca Pb, Nd, etc.) depending on the composition exhibits various physical, optical, and magnetic phenomena exists in these materials due to the Jahn-Teller distortion, double exchange depending on the composition. Doped lanthanum manganites can be used in storage technologies, biomedical applications, micro electrical devices, solid oxide fuel cells, magnetic hyperthermia [1-3]. These materials are utilized to create cooling systems that have a high cooling efficiency while producing minimal noise, emit no greenhouse gases and are environmentally beneficial [4,5].

The parent compound $LaMnO_3$ was regarded as the standard Jahn-Teller (JT) system with deformation of tetragonal structure in MnO6 octahedra [6]. The alternate short and long Mn- O bonds make its structure. An efficient hole doping was accomplished by replacing trivalent La ion by divalent Sr ion. The double exchange interaction between the ions occurs due to the change in the oxidation state from Mn^{3+} to Mn^{4+} by the doping with divalent Sr ion. The ionic radii of A and B sites and Mn^{3+} to Mn^{4+} ratio effects the bond length (Mn-O) and bond angle (Mn-O-Mn), thereby varying the double exchange interaction. Due to this, structural and magnetic properties of doped Lanthanum manganites were strongly affected [7]. The characteristic behavior of these manganites drastically changes due to the concentration of substitution at La site [8-13]. Lanthanum doped perovskite type manganite are fascinating and demanding materials because of these characteristics. With the rapid integration and downsizing of electronic devices, these perovskite manganites are prepared in nanoscale. These Strontium doped lanthanum manganite $La_{1-x}Sr_xMnO_3$ have more advantages than typical magnetic materials with regards to its optical and magnetic parameters.

The physical characteristics perovskite manganite influenced by the synthesis process, size, symmetry of unit cell, dopant etc. [14-16]. The relationship among structural, orbital, and electronic degrees of can be explored further to fully comprehend the complicated science behind rare – earth manganite features. The annealing temperature can affect grain size, therefore increasing the annealing temperature should increase grain growth [17,18]. Due to its intriguing properties, like huge ratio between surface to volume and surface effect, research on perovskite manganite with nanoscale particle sizes has grown in recent years.

The nanoscale manganites have novel characteristics which vary with particle size when compared to those bulk materials. Because manganite nanoparticles are primarily metal conductors, only a few prior research have been done on their optical characteristics. The combustion method has been used in this research to synthesize nanocrystallites because of its convenience of use, low cost, and modest annealing temperature for nanocrystallites. This method also enables the production of nanocrystallites on a massive scale, down to tenths of a gram. The nanocrystallites were annealed at different temperatures to better understand the impact of

temperature on characteristics. However, some research has been carried out on strontium doped lanthanum nanoparticles and not comprehensively considered the dopant concentration x = 0.75 on the structural, optical properties of $La_{1-x}Sr_xMnO_3$ at different annealing temperatures. In this present work, the preparation, the size dependence of structural and optical properties $La_{0.25}Sr_{0.75}MnO_3$ perovskite nanocrystallites were reported at annealed temperatures 600, 800,1000 and 1200℃.

MATERIALS AND EXPERIMENTAL

The $La_{0.25}$ $Sr_{0.75}$ MnO_3 nanocrystallites were prepared using combustion process with their nitrate precursors of Lanthanum [$La(NO_3)_3.6H_2O$], Strontium and Manganese [$Sr(NO_3)_2$] and [$Mn(NO_3)_2.4H_2O$] of 99.98% purity AR grade compounds. These starting compounds with their stoichiometry were separately dissolved in de-ionized water and mixed in a beaker to form a desired precursor solution. The citric acid ($C_6H_8O_7$) in a stoichiometric volume was mixed with precursors solution for initiating the reaction. The molar ratio of citric acid and nitrate ions are set to 1:3. To maintain pH level 7, ammonia was added drop by drop until the solution becomes thick brown color. To gel the solution ethylene glycol in stoichiometric volume was added. This aqueous solution was placed on a magnetic stirrer and stirred continuously keeping the temperature about 80℃ until it converts into a viscous gel. Thereafter the solution was heated at about 300℃ until an auto combustion was initiated.

After auto combustion, a free dark powder is obtained [19]. The obtained powder was grounded and divided in to four parts and annealed separately at 600, 800, 1000 and 1200℃ for 6 hours. Finally, $La_{0.25}Sr_{0.75}MnO_3$ various sized nanocrystallites were obtained. The annealed powders were mixed fine with 1.5% PVA which acts as a binder. Then it was pressed at a pressure of 5 tons per cm^2 until the pellets of 10mm in diameter and 2-3 mm thick. These pellets were annealed at 600, 800, 1000 and1200℃ for 4 h. The structural properties were calculated by using the X-ray powder diffraction (XRD) with incident radiation of CuKλ (λ = 1.5418 Å) using Rigaku (Miniflex-II) diffractometer with step size of 0.02° and 2θ angular range from 20° to 80°. Variation of absorbance as a function of wavelength was evaluated by the UV-Vis Spectroscopy (SYSTRONICS DOUBLE BEAM).

RESULT AND DISCUSSION:

X ray diffraction Analysis: The XRD spectra of $La_{0.25}Sr_{0.75}$ MnO_3 nanocrystallites annealed at temperatures 600, 800,1000 and 1200℃ were presented in figure 1. All identified peaks were matched with JCPDS (00-056-0616) card. From figure1, the formation of Rhombohedral structure with space group of $R\bar{3}C$ with no impurities were confirmed by the XDR patterns. The distinctive XRD peaks with large full width half maximum reveal the formation of nanocrystals. The intensity of prominent peak for 1200℃ formed for $La_{0.25}$ $Sr_{0.75}$ MnO_3 perovskite structure is substantially higher than others because of the high electron density, attributed to the large crystallite size.

The crystallite sizes were measured using Debye - Scherrer relation.

$$D = \frac{k\lambda}{\beta \cos\theta} \dots\dots\dots\dots\dots (1)$$

Where D, k, λ, β are represents the average crystalline size, shape factor (0.9), wavelength of ray radiation (1.5418Å) and full width half maximum respectively.It was observed that FWHM values were decreased, whereas the average crystallite sizes were increased with the rise in annealed temperature which are shown in Table 1. Micro strain values are calculated from the equation [20].

$$\varepsilon = \frac{\beta}{4\tan\theta} \quad \dots\dots\dots\dots\dots (2)$$

It has been observed that the micro strain was reduced with the raise in annealed temperature from 600 to 1200℃.

The dislocation densities were calculated using the following equation [20].

$$\delta_D = \frac{1}{D^2} \dots\dots\dots\dots\dots\dots (3)$$

The measured values of dislocation density were decreased from 5.38 $\times 10^{-3}$ to $1.94\times 10^{-3} nm^{-2}$ with increase in annealed temperature from 600 to 1200℃.

Table 1: Structural and Optical parameters of the $La_{0.25}Sr_{0.75}MnO_3$ nanoparticles annealed at 600, 800,1000 and 1200℃.

Annealed Temperature	**600**℃	**800**℃	**1000**℃	**1200**℃
Crystallite Size D (nm)	13.62	14.82	19.00	22.70
Dislocation density (δ_D) (nm^{-2}) $\times 10^{-3}$	5.38	4.55	2.76	1.94
Micro strain (ε)$\times 10^{-3}$	9.03	8.22	6.41	5.36
Absorption peak U-V region (nm)	240	220	215	214
Absorption peak Visible region (nm)	453	455	467	468
Band gap (eV)	3.83	3.14	2.89	2.64

UV-Vis spectroscopic analysis:

The main physical features that describe the optical properties of $La_{0.25}Sr_{0.75}MnO_3$ nanocrystallites are the energy gap and refractive index of perovskite manganites. UV-Visible absorption spectra of $La_{0.25}Sr_{0.75}MnO_3$ nanocrystallites annealed at temperatures 600,800,1000 and 1200℃ were measured in the wavelength range 200-800nm with a step size of 0.2nm. The variation of absorbance of all the samples were obtained from the Ultraviolet -Visible spectrometer. figure 2(a) reveals that maximum sharp absorption band in the UV-Vis was identified in the range 214-220nm in ultraviolet region for $La_{0.25}Sr_{0.75}MnO_3$ nanocrystallites annealed at temperatures 600, 800, 1000 and 1200℃ and maximum absorption edge was also found in the range 453-458nm in the visible region. From figure 2(a) it has been noticed that the absorption decreases in the visible region for all prepared samples. It has also been noticed that maximum absorption band in the UV range decreases as the annealed temperature increases, whereas maximum absorption band in the Visible range increases with the annealed temperature.

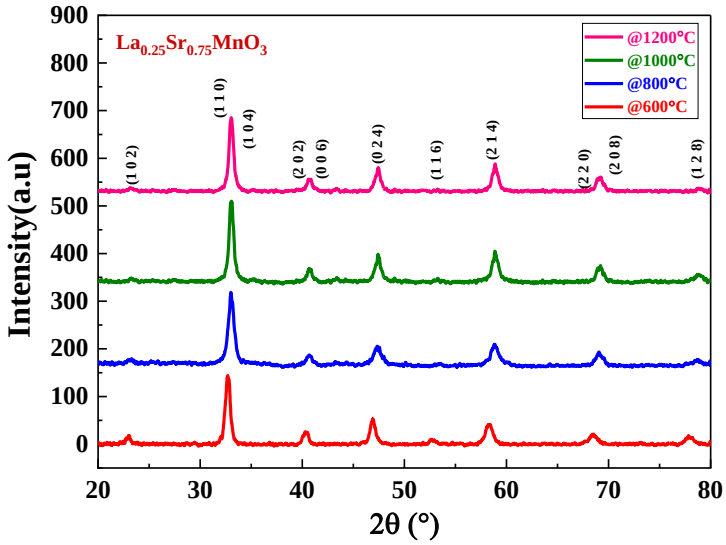

Figure 1: XRD pattern for the $La_{0.25}Sr_{0.75}MnO_3$ nanocrystallites annealed at 600, 800, 1000 and 1200°C.

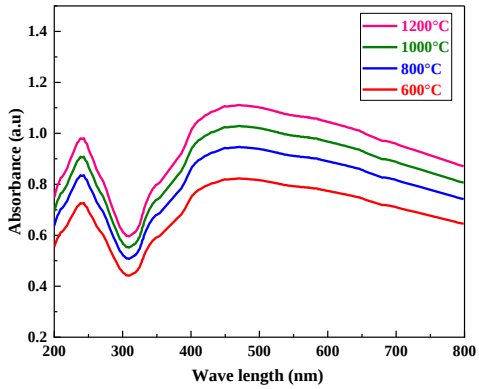

Figure 2(a)

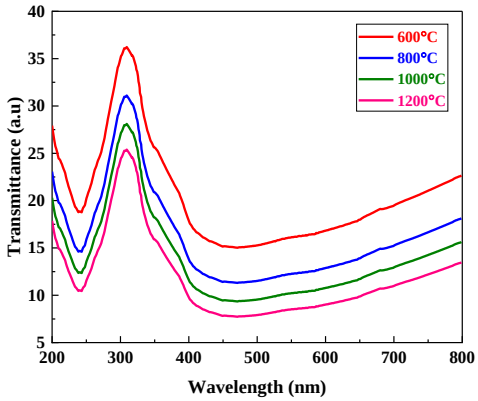

Figure 2(b)

Figure 2(a-b): UV-Vis Absorbance spectra and Transmittance spectra of the $La_{0.25}Sr_{0.75}MnO_3$ nanocrystallites annealed at 600, 800, 1000 and 1200°C.

Beer-Lambert's Law was used to calculate the absorption coefficient of $La_{0.25}Sr_{0.75}MnO_3$ nanocrystallites [21,22].

$$I = I_0 e^{\alpha t} \dots\dots\dots\dots\dots\dots (4)$$

$$A = log\left(\frac{I_0}{I}\right) \dots\dots\dots\dots\dots\dots (5)$$

$$\alpha = \frac{2.303\ A}{t} \dots\dots\dots\dots\dots\dots\dots (6)$$

Where I_0 = Incident intensity; I = Transmitted intensity, α = Absorption coefficient; A= Absorbance and t = thickness of the sample (1cm) respectively.
The transmittance (T_s) can be evaluated from the relation.

$$T_s = 10^{-A} \times 100 \dots\dots\dots\dots\dots (7)$$

The variation of transmittance with wavelength of all samples was predicted in figure 2(b)The dynamic refractive index was measured using the below relation.

$$n = \frac{1}{T_s} + \sqrt{\frac{1}{T_s - 1}} \dots\dots\dots\dots\dots\dots\dots (8)$$

where *n* and Ts represent the refractive index and the transmittance.

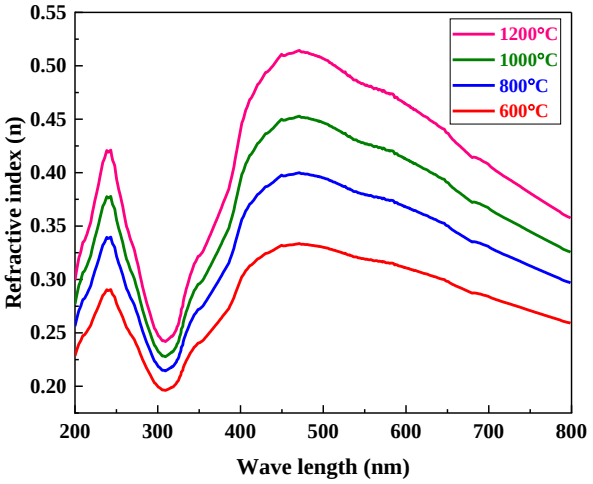

Figure 3: Variation of refractive index with the wavelength of the $La_{0.25}Sr_{0.75}MnO_3$ nanocrystallites annealed at 600, 800, 1000 and 1200℃.

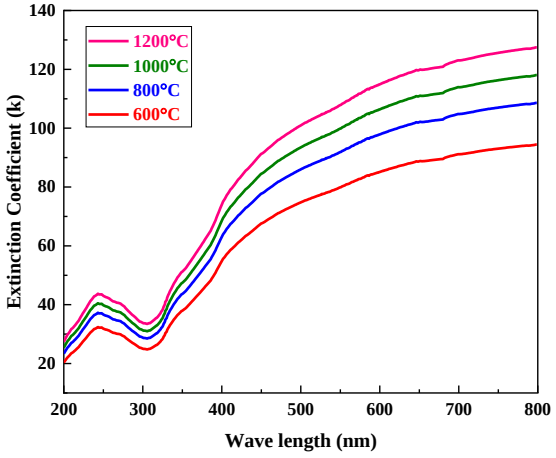

Figure 4: Variation of extinction coefficient of the $La_{0.25}Sr_{0.75}MnO_3$ annealed at 600, 800, 1100 and 1200℃.

Variation of refractive index with the wavelength of all $La_{0.25}Sr_{0.75}MnO_3$ nanocrystallites were shown in Figure 3. It has been noticed that the refractive index of all $La_{0.25}Sr_{0.75}MnO_3$ nanocrystallites increases, becomes maximum at around 240nm and decreases in the region 240-340nm. After 340nm, the refractive index increases up to around 460nm then decreases. The dynamic refractive index values are in the range 0.19 to 0.51 for all samples and the minimum refractive index value 0.19 has identified at wavelength 309nm for the photon energy of 4.06eV. The maximum refractive index value has been found at 460nm for the photon energy 2.65eV.

Extinction coefficient of all $La_{0.25}Sr_{0.75}MnO_3$ nanocrystallites were measured using the relation [23].

$$k = \frac{\alpha\lambda}{4\pi} \dots\dots\dots\dots\dots\dots\dots\dots (9)$$

where 'k' is the extinction coefficient and 'α' is the absorption coefficient.

The variation of extinction coefficient with wavelength was shown in figure 4. From figure 4, it has been observed that the variation of extinction coefficient increases from 20 to 250nm, then decreases and becomes minimum around 330nm.After 350nm extinction coefficient increases exponentially with the annealing temperature.

The reflectance of $La_{0.25}Sr_{0.75}MnO_3$ nanocrystallites were evaluated with the values of refractive index as given by the expression [24].

$$R = \frac{(n-1)^2}{(n+1)^2} \dots\dots\dots\dots (10)$$

The variation of reflectance with wavelength is shown in figure 5.

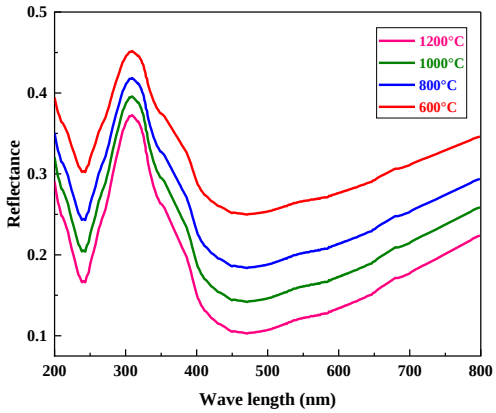

Figure 5: Variation of reflectance of the $La_{0.25}Sr_{0.75}MnO_3$ annealed at 600, 800, 1000 and 1200°C.

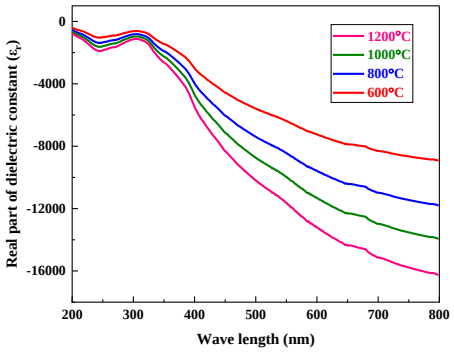

Figure 6(a)

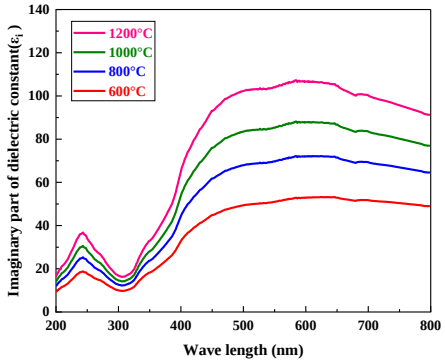

Figure 6(b)

Figure 6(a-b): Variation of real and imaginary part of dielectric constant of the $La_{0.25}Sr_{0.75}MnO_3$ annealed at 600, 800, 1000 and 1200°C.

The reflectance value increases to maximum value and then falls in the 200-300nm range whereas it increases in the visible range. The maximum reflectance value has been identified around wavelength 306nm.

The real and imaginary part of dielectric constants can be measured using the relations [25,26].

$$\varepsilon_i = 2nk \dots\dots\dots\dots\dots (11)$$

$$\varepsilon_r = n^2 - k^2 \dots\dots\dots\dots\dots\dots (12)$$

The variation of real and imaginary part of dielectric constants with wavelength was shown in figure 6(a-b). It was noticed that, for the $La_{0.25}Sr_{0.75}MnO_3$ nanocrystallites, the real part of dielectric constant values decreases while imaginary part of dielectric constant increase in a nonlinear manner with increasing wavelength.

The band gap of post annealed $La_{0.25}Sr_{0.75}MnO_3$ nanocrystallites were measured using Tauc's relation and obtained by Tauc plots [22].

$$(\alpha h\nu)^n = A\left(h\nu - E_g\right) \dots\dots\dots\dots\dots (13)$$

Where E_g, h, υ, n is the optical band gap, planck's constant, frequency, and index parameter respectively. 'n' represents the nature of electron band transition. There are 4 possible values of 'n' depending upon the type of the transition which relates n =1/2 (permissible indirect), n=1(forbidden indirect), n=3/2(forbidden direct), and n=2 (allowed direct) [27]. The Tauc plots of $(\alpha h\nu)^n$ versus photon energy (hν) for different 'n' values for $La_{0.25}Sr_{0.75}MnO_3$ nanocrystallites were plotted. Among all the plots $(\alpha h\nu)^2$ verses (hν) plot has a linear relationship over a wide range as observed, indicates the system take the direct transition in the broad band gap area. The optical band gap of all the $La_{0.25}Sr_{0.75}MnO_3$ nanocrystallites were reported in figure 7 by the extrapolating the proportionality section of the graph on the x-axis. The direct band gap values for $La_{0.25}Sr_{0.75}MnO_3$ post annealed nanocrystallites are provided in Table 1, suggests that optical gap reduces from 3.83 to 2.64eV with the increase of annealed temperature. So, because the variation of band gap was a function of annealed temperature (red shift) can be ascribed to increase in particle size, which was correlated to XRD results. The prepared samples are found to be great choices for photocatalytic activities based on the band gap energy values.

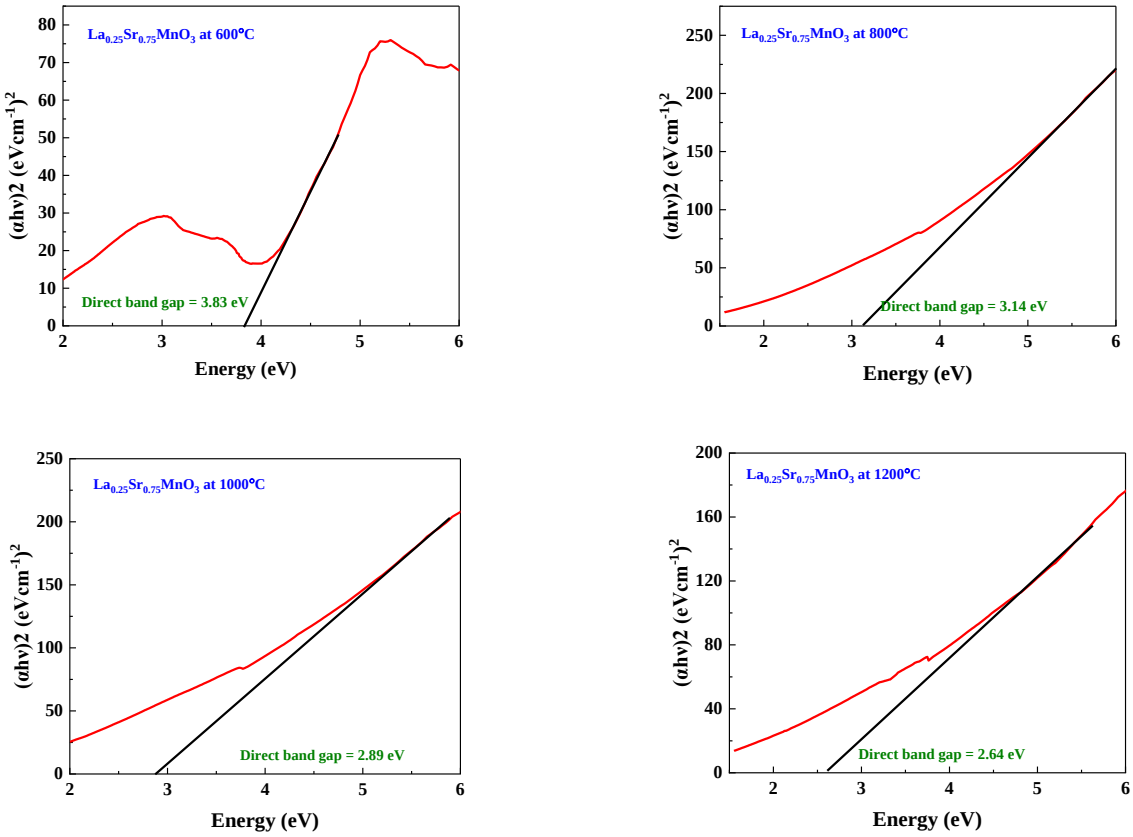

Figure 7: UV-Vis absorbance -Tauc plot: $(\alpha h\nu)^2$ verses hν of the $La_{0.25}Sr_{0.75}MnO_3$ nanocrystallites annealed at 600, 800, 1000 and 1200°C.

CONCLUSIONS:

1.The $La_{0.25}Sr_{0.75}MnO_3$ nanocrystallites were successfully synthesized using the method of combustion and annealed to get various crystallite sizes.
2.The X ray diffraction confirmed the formation of Rhombohedral structure with space group $R\bar{3}c$ without any impurity peaks.
3.The crystallite sizes of $La_{0.25}Sr_{0.75}MnO_3$ nanocrystallites peak increases from 13.62 to 22.70nm as function of annealed temperature.
4.The dynamic refractive index values are in the range 0.19 to 0.51 for all $La_{0.25}Sr_{0.75}MnO_3$ samples.
5.UV-vis spectroscopic studies showed that the band gap values changed from 3.83 to 2.64eV as nanocrystallites size increased, indicating that $La_{0.25}Sr_{0.75}MnO_3$ nanocrystallites were semiconductors in nature.

ACKNOWLEDGEMENTS

The authors expressed their thankfulness to the Principal, JNTUH University College of Engineering Rajanna Sircilla, the Principal, SRR Government Arts & Science College (Autonomous), Karimnagar and the Chairman, Marri Laxman Reddy Institute of Technology and Management, Hyderabad for their constant support in carrying out this research work.

REFERENCES

[1]N.D. Thorat, R. Bohara, Multifunctional magnetic nanostructures for cancer hyperthermia therapy, in Alina Maria Holban, Alexandru Grumezescu (Eds), Nanoarchitectonics for Smart Delivery and Drug Targeting, William Andrew, App.Sci. Publishers,2016, pp.589-612.
[2]N. Abdul Jaffar, K.B, Lias, N. Buniyamin, An overview of metametrials used in applicators in hyperthermia cancer treatment procedure, IEEE International Conference on Electrical, Electronics and System Engineering (ICEESE), 2017, pp.32-36.
[3]N. Nizam-Uddin, Ibrahim Elshafiey, SAR optimization for wideband hyperthermia treatment system, IEEE 8th International Conference on Information Technology (ICIT),2017, PP.956-959.
[4]A. Gaur, G.D. Varma, Sintering temperature effect on electrical transport and magnetoresistance of nanophasic La0.7Sr0.3MnO3. J Phys. Condens Matter, 14(2006) 8837-8846.
[5]S. Zhao, X.-J. Yue, X. Liu, Influence of Sr doping on structural, electric, and magnetic properties of La0.7Ca0.3MnO3 nanoparticles, Ceram Int, 43(2017) 13240-13246.
[6] J. B. Goodenough, Phys. Rev. B,1955, 100, 564-573.
[7]N. Zaidi, S. Mnefgui, A. Dhatri, Dhahri, E.K. Hlil, J. Alloys Compd.616(2014) 378-384.
[8]H. Nakatsugawa, M. Saito, and Y. Okamoto," High-temperature thermoelectric properties of perovskite – type Pr0.9Sr0.1Mn1-xFeO3(0 □ x □ 1)," Journal of Electronic materials, Vol.46, pp.3262-3272,217.
[9]Y. Tokura, "Critical features of colossal magnetoresistive manganites," Report on Progress in Physics, vol.69, pp.797,2006.
[10]C.B. Larsen, S. Samothrakitis, A.D. Fortes, A.O. Ayas, M. Akyol, A. Ekicibil, and M. Laver, "Basal plane ferromagnetism in the rhombohedral manganite La0.85Ag0.15MnO3+□," Journal of Magnetism and Magnetic Materials, vol.498, p.166193,2020.
[11]M.K. Verma, N.D. Sharma, S. Sharma, N. Choubhary, and D. Singh, "High magnetoresistance between their magnetic and electrical properties," Materials Research Bulletin, vol.125 pp.10813,2020.
[12]S. Biswas, and S. Keshri," Large magnetocaloric near room temperature in La0.67(Sr, K/Pb)0.33MnO3 manganite nanomaterials," Journal of Materials Science: Materials in Electronics, vol pp.21896-21912,2020.
[13]L. Joshi, S.S. Rajput, and S. Keshri," Structural and magneto transport properties of LCMO-STO composites." Phase Transition, vol.83, pp.482,2010.
[14]R.V. Helmholt, J. Wecker and B. Holzapfel, Phys. Rev.Lett.,1993,71,2331-2333.
[15]K. Chahara, T. Ohno and M. Kasai, Appl. Phys. Lett., 1993,63,1990-1992.
[16]S. Jin, T.H. Tiefel, and M. McCormack, Scince,1994,264,413-145.
[17]M. Oumezzine, O. Pena, T. Guizouarn, R. Lebullenger, M. Oumezzine, Impact of the sintering temperature on the structural, magnetic, and electrical transport properties of doped La0.67 Ba0.33 Mn0.9 Cr0.1O3 manganite, J Magn Magn Mater,324(2012) 2821-2828.
[18]M. Rosic, L. Kljaljevic, D. Jordanov, M. Stoiljikovic, V. Kusigerski, V Spasojevic, B. Matovic, Effects of sintering on the structural, microstructural, and magnetic properties of nanoparticles manganite Ca1-x GdxMnO3 (x = 0.05,0.1,0.15,0.2,), Ceram Int, 41(2015) 14964-14972.
[19]Weiren Xia, Kai Leng, Oingkai Tang al. Comparative studies on the structural, magnetic, and optical properties of perovskite Ln0.67Ca0.33MnO3 (Ln = La, Pr, Nd, and Sm) manganite nanoparticles synthesized by sol-gel method: AIP Advance 11,035007 (2021).
[20]Pawar, D.K. Pawar, S.M., Patil, P.S. and Kolekar, S.S. (2011) Synthesis of Nano- crystalline Nickel – Zinc Ferrite (Ni0.8Zn0.2Fe2O4) Thin Films by Chemical Bath De-position Method. Journal of Alloys and Compounds, 509,3587-3591.
[21]Pathan, H.M., Desai, J.D. and Lokhande, C.D. (2002) Modified Chemical Deposition and Physico- Chemical Properties of Copper Sulphide (Cu2S) Thin Films. Applied Surface Science, 202,47-56.

[22]Srivastava, M., Ojha, A.K., Chaubey, S. and Materny, A. (2009) Synthesis and Optical Characterization of Nanocrystalline NiFe2O4 Structures. Journal of Alloys and Compounds, 481,515-519.

[23]Xue, S.W., Zu, X.T., Zhou, W.L., Deng, H.X., Xiang, X., hang, L. and Deng H. (2008) Effects of Post- Thermal Annealing on the Optical Constants of ZnO Thin films. Journal of Alloys and Compounds,448, 21-26.

[24]Ashour, A., El-Kadry, N. and Mahmoud, S.A. (1995) On the Electrical and Optical Properties of CdS Films Thermally Deposited by a modified Source. Thin Solid Films, 269,117-120.

[25]Greenaway, D.L. and Habeke, G. (1968) Optical and Band Structure of Semiconductors. Pergamon, New York.

[26]Guneri, E and Kariper, A. (2012) Optical Properties of Amorphous CuS Thin Films Deposited Chemically at Different pH values. Journal of Alloys and Compounds, 516,20-26.

[27]U. Kumar, D. Yadav, S. Upadhyay, Investigation of structural, optical, and magnetic properties of Nd-doped Sr2SnO4 Ruddlesden Popper oxide. J Am Ceram Soc 103,5743- 5757(2020).American cancer society. Cancer facts and figures, 1994. Atlanta: American Cancer Society, 1994; publication no. 5008.94